J. Sound Vib. (1970) **11** (1), 3–18

THE ROLE OF DAMPING IN VIBRATION THEORY

S. H. CRANDALL

Department of Mechanical Engineering, Massachusetts Institute of Technology, Cambridge, Massachusetts, U.S.A.

(*Received* 28 *July* 1969)

In many applications of vibration and wave theory the magnitudes of the damping forces are small in comparison with the elastic and inertia forces. These small forces may, however, have very great influence under certain special circumstances. Damping arises from the removal of energy by radiation or dissipation. It is generally measured under conditions of cyclic or near-cyclic motion. The nature of some important damping mechanisms is discussed and an indication is given of how the damping depends on the amplitude and frequency of the cyclic motion. The idealized models of damping which are commonly employed in theoretical analyses are described and some limitations are noted. Damping is of primary importance in controlling vibration response amplitudes under conditions of steady-state resonance and stationary random excitation. Damping also plays a crucial role in fixing the borderline between stability and instability in many dynamical systems. Some examples which illustrate this are discussed, including shaft whirl, and pipeline flutter.

1. INTRODUCTION

The central phenomenon of vibration theory is cyclic oscillation. A major feature of oscillation dynamics is the cyclic transformation of potential energy into kinetic energy and back again. This feature is clearly displayed by idealized models involving only elastic and inertial elements. For example the natural frequencies and natural modes of vibrating systems and the group and phase velocities of wave propagating systems are obtained from such idealized models. Secondary aspects of oscillation dynamics can be explained by accounting for a *damping* mechanism, i.e. a mechanism which removes energy from the oscillating system under consideration. Damping is responsible for the eventual decay of free vibrations and provides an explanation for the fact that the response of a vibratory system excited at resonance does not grow without limit.

One purpose of the present paper is to review some of the properties of actual damping mechanisms and to describe some of the mathematical models that are employed to represent these mechanisms. A second purpose is to draw attention to those special circumstances where small amounts of damping have an exaggerated importance in determining the dynamic behavior of a system.

2. THE NATURE OF DAMPING

Damping is the removal of energy from a vibratory system. The energy lost is either transmitted away from the system by some mechanism of radiation or dissipated within the system. Most measurements of damping are performed under conditions of cyclic or near cyclic oscillation. Commonly the decay of free oscillation is observed or measurements are made of steady-state forced vibration at (or in the vicinity of) resonance. In both cases the total energy W removed in a cycle can be inferred but the measurements are seldom precise

enough to provide a detailed picture of how the instantaneous rate of energy removal fluctuates within a single cycle. If the oscillation of the system is in a single well-defined mode whose amplitude is characterized by a and whose frequency is ω, the energy lost per cycle generally varies with both a and ω, i.e. $W = W(a, \omega)$.

A convenient measure of damping is obtained by comparing the energy lost in a cycle with the peak potential energy V stored in the system during that cycle. The *loss factor* η is defined as

$$\eta = \frac{W}{2\pi V}. \tag{1}$$

If the energy could be removed at a uniform rate throughout a cycle of simple harmonic motion (such a mechanism is not actually very likely) then $W/2\pi$ could be interpreted as the energy loss per radian and η would be simply the energy loss per radian divided by the peak energy available.

In most dynamic systems which are of interest from the point of view of vibrations the damping is small. The values for loss factor that are encountered in practice range from about $\eta = 10^{-5}$ to $\eta = 2 \times 10^{-1}$; although larger values of η are found in instrument mechanisms, transducers and vehicle suspensions. In general the loss factor η depends on both the amplitude and frequency of the oscillation. If, however, the system is completely *linear*, then both W and V are proportional to a^2 and the loss factor η is *independent* of amplitude. For linear damping mechanisms the loss factor generally has an important frequency dependence.

These ideas can be illustrated by considering a bar of aluminum alloy suspended by strings as shown in Plate 1. Once the bar is set into bending vibration by a blow, it generates a sound with a fundamental frequency of 130 Hz which remains audible for several seconds as the vibration decays. The (measured) loss factor at this frequency is $\eta = 1{\cdot}5 \times 10^{-3}$. There are several damping mechanisms contributing to the total energy removed each cycle. The very fact that the vibration is audible is an indication that there is acoustic radiation away from the bar. There is undoubtedly some radiation of energy up the supporting strings even though they are attached at the nodal points of the fundamental bending node. There is also dissipation of energy within the aluminum. Even in a system as simple as this it is difficult to account quantitatively for all the damping.

Rough estimates can sometimes be made of the amounts of damping contributed by internal dissipation and by acoustic radiation. A great many linear and non-linear mechanisms of internal damping in metals have been identified [1, 2]. For aluminum in bending at room temperature the major contribution is made by transverse heat flow from the warmed compression fibers to the cooled tension fibers. This is a linear relaxation mechanism which depends on the temperature T, the thermal expansion coefficient α, the conductivity κ, and the specific heat c_v of the beam as well as on its thickness h, modulus E and frequency f of oscillation. In Figure 1 the loss factor predicted by this mechanism alone is compared with measured total internal loss factors of cantilever specimens. For the beam in Plate 1 the relaxation frequency is $f_0 = 7{\cdot}5$ Hz and the total internal loss factor for vibration in the fundamental mode can be estimated to be about $3{\cdot}5 \times 10^{-4}$.

The general nature of the acoustic radiation from a vibrating beam is known [5] but a quantitative analysis for the radiation from the lower modes appears to be beyond the present state of the art. A number of investigators [6, 7, 4, 8] have measured the air damping of thin cantilever beams. For large bending amplitudes air damping is non-linear, the loss factor increasing roughly in proportion to the amplitude. For small amplitudes the air damping loss factor appears to approach a limit which is independent of amplitude. This small amplitude loss factor appears to depend only on the ratio of the cantilever length L to the beam thickness h as shown in Figure 2. If the beam of Plate 1 had been supported as a cantilever

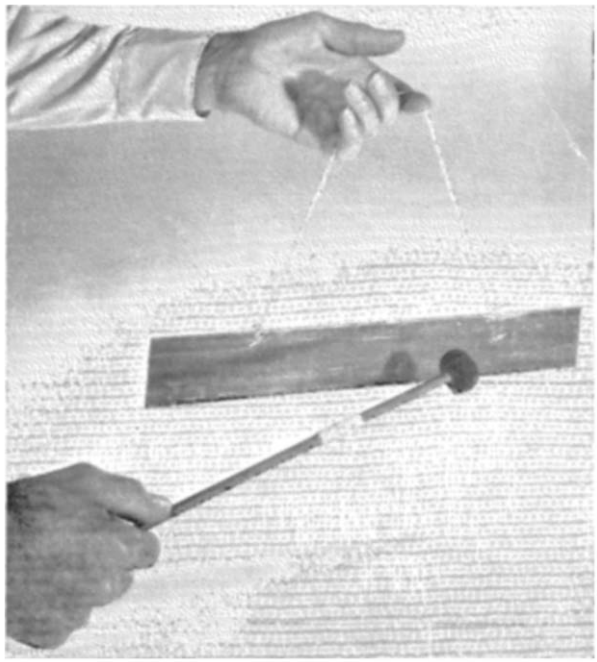

Plate 1. Vibrating beam suspended in air is damped by radiation up strings, acoustic radiation and internal damping within bar.

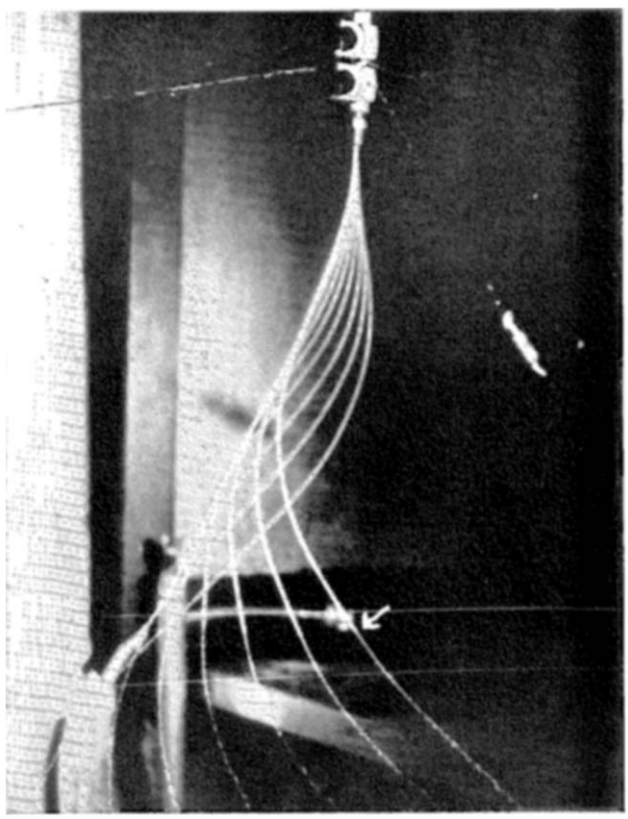

Plate 2. Strobe sequence of fluttering tube, eight flashes during half a cycle. Arrow marks end of tube. From [34].

(*facing p. 4*)

beam, its fundamental frequency would have been 21 Hz with an acoustic radiation loss factor of $1{\cdot}6 \times 10^{-4}$ according to Figure 2. Unfortunately similar loss-factor information is not available for the fundamental free-free mode.

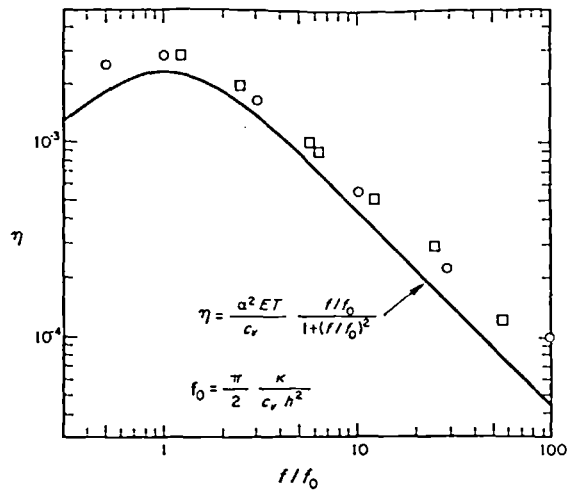

Figure 1. Loss factor as function of frequency. Comparison of measured values of internal damping for 2024-T4 cantilever beams with theoretical loss factor due to transverse heat flow. Adapted from [3].

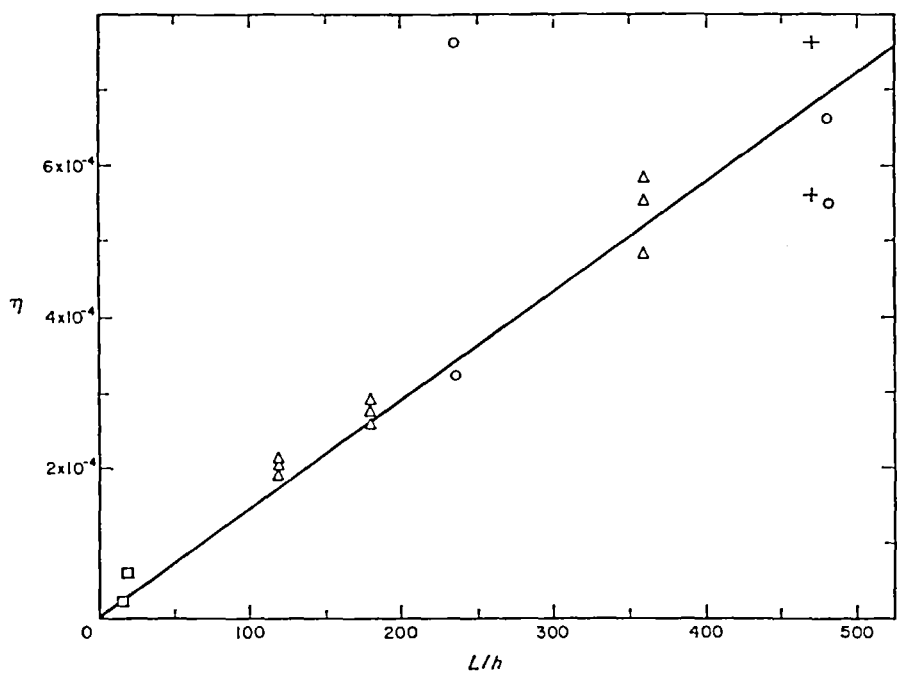

Figure 2. Low-amplitude air-damping loss factor for fundamental mode of thin cantilever beams as a function of length-thickness ratio. Adapted from [8].

The radiation damping of a system can be altered by changing the coupling with the exterior. The internal damping in a system can be altered by introducing energy absorbing devices. The beam in Plate 1 can be used to illustrate these statements. The radiation damping can be greatly increased if instead of supporting the beam by strings we clamp it to a desk.

Vibrational energy, which at first is localized within the beam, is rapidly transmitted throughout the larger structure. This energy transfer within the beam-desk system is counted as an energy loss for the beam considered as an isolated system. The internal damping of the beam can be increased by changing the beam material for aluminum to stainless steel (for example) or by adding damping tape or other acoustical coatings which utilize a viscoelastic material to dissipate energy. For example, Figure 3 shows how the loss factors of the first five modes

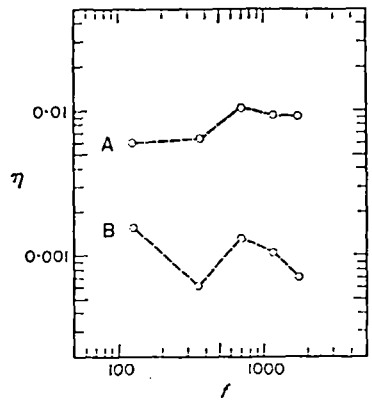

Figure 3. Loss factors for first five modes of free-free beam. A, After and B, before, applying damping tape.

of the beam in Plate 1 are increased by applying a $1\frac{3}{4}$ in. × 13 in. strip of damping tape (3-M No. 425 tape which consists of aluminum foil 0·003 in. thick and a layer of adhesive 0·002 in. thick) to one side of the $\frac{1}{8}$ in. thick beam whose face dimensions are 2 in. × $14\frac{5}{16}$ in.

Both radiation damping and internal dissipation can be expected to be frequency dependent. If the radiation is to a linear external system the loss factor will be affected by the frequency response of the external system. If the internal dissipation is due to a linear relaxation mechanism there will be a pronounced increase in loss factor when the oscillation frequency approaches the relaxation frequency.

3. MATHEMATICAL MODEL OF DAMPING

The prototype for a lossless vibration system is the simple spring-mass model shown in Figure 4(a). The natural free vibration is simple harmonic motion with frequency $\omega_n = \sqrt{k/m}$. When the exciting force is a steady-state sinusoid with frequency ω there is a steady-state sinusoidal solution for the motion which has the same frequency ω and has a finite amplitude if $\omega \neq \omega_n$. This model possesses many characteristics of actual physical systems but suffers from the following drawbacks. The free vibration, once excited, never decays. When excited at resonance ($\omega = \omega_n$) by a steady-state sinusoid applied at $t = 0$ the predicted response is an oscillation whose amplitude grows linearly with t, i.e. a steady state is never achieved. When excited by a stationary random force whose spectrum includes ω_n the response is a non-stationary random process [9] whose r.m.s. level grows essentially in proportion to $\sqrt{t}$; i.e. a stationary state is never achieved.

The classical remedy for these drawbacks is to introduce an ideal linear dashpot into the model as shown in Figure 4(b). It is assumed that the dashpot exerts a force $f_d = cv$ in opposition to a relative velocity v across its terminals. The constant c is called the dashpot parameter. The free vibration in this case is a damped oscillation and there is a finite steady-state response

to any steady-state sinusoidal excitation. There is also a stationary random response process for any stationary excitation process.

Let us examine the ideal linear damper more closely. Suppose that a steady-state simple harmonic motion $x = a\cos\omega t$ is established in Figure 4(b). The energy W dissipated in a cycle is

$$W = \int_0^{2\pi/\omega} \left(c\frac{dx}{dt}\right)\frac{dx}{dt}dt = \pi c a^2|\omega| \tag{2}$$

while the peak potential energy stored in the spring during the cycle is

$$V = \tfrac{1}{2}ka^2. \tag{3}$$

The loss factor for the ideal damper in the system of Figure 4(a) is thus

$$\eta = \frac{c|\omega|}{k} \tag{4}$$

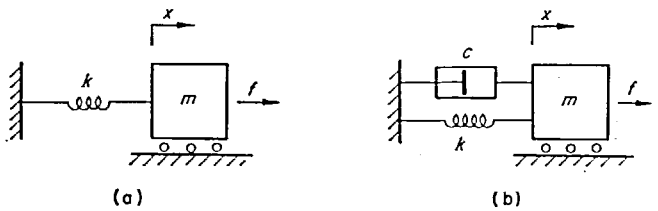

Figure 4. Ideal single-degree-of-freedom vibration models. (a) Lossless model, (b) model with ideal viscous damper.

according to (1). We may note that the absolute value signs on ω are required in (2) since the motion $x(t)$ itself, as well as the energy loss per cycle, is not affected by changing the sign of ω. Thus, considered as functions of ω, the energy loss per cycle W and the loss factor η are real, non-negative, and even.

In many applications where the damping is light the affect of damping is appreciable only for resonant or near-resonant motions. These effects can be described in terms of the loss factor at resonance ($\omega = \omega_n$)

$$\eta_n = \frac{c\omega_n}{k} = \frac{c}{\sqrt{km}}. \tag{5}$$

Thus the free vibration of the system of Figure 4(b) has the form

$$x(t) = a_0 e^{-1/2\eta_n\omega_n t}\cos(\omega_d t + \phi_0) \tag{6}$$

where $\omega_d^2 = \omega_n^2(1 - \eta_n^2/4)$ and the amplitude a_0 and phase ϕ_0 depend on the initial conditions. Note that the rate of envelope decay depends on η_n. The logarithmic decrement is

$$\delta = \log\frac{x(t)}{x(t + 2\pi/\omega_d)} = \pi\eta_n\frac{\omega_n}{\omega_d} = \frac{\pi\eta_n}{\sqrt{1 - \eta_n^2/4}}. \tag{7}$$

When the exciting force in Figure 4(b) is a steady-state sinusoid $f = F\sin\omega t$ the steady-state response is

$$x = X\sin(\omega t + \phi) \tag{8}$$

where the response amplitude X depends on the frequency ω and on the resonant loss factor η_n as indicated in Figure 5. Note that for light damping the response amplitude is substantially independent of the damping except in the vicinity of $\omega = \omega_n$ where it depends critically on

η_n. We can also infer from Figure 5 that the spectral density of the response to a stationary random exciting force depends critically on the resonant loss factor.

In section 2 it was suggested that most linear damping mechanisms have considerable frequency dependence. In many cases, however, the frequency dependence of actual loss factors bear little relation to equation (4) for the ideal dashpot. Nevertheless for many purposes the actual damping can be modelled satisfactorily by an equivalent dashpot. This is indicated in Figure 6 where the frequency dependence of an actual loss factor in a single-degree-of-freedom oscillator is compared with that of an ideal dashpot. If the dashpot is

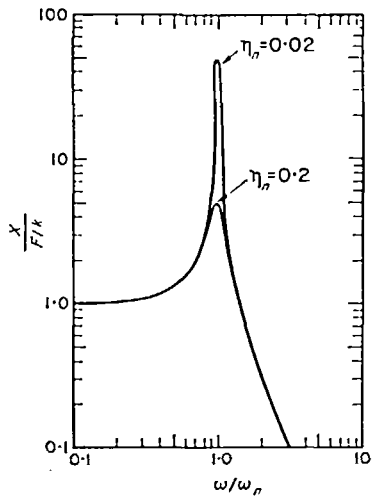

Figure 5. Steady-state frequency response of single-degree-of freedom oscillator with ideal linear dashpot.

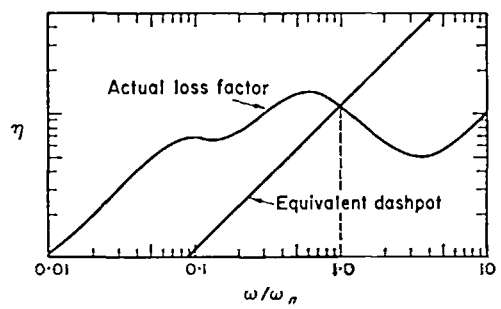

Figure 6. Frequency dependence of actual loss factor and loss factor of equivalent ideal dashpot.

selected so that its loss factor is the same as the actual loss factor at the natural frequency of the oscillator the behavior of the model will be sufficiently close to that of the actual system for most purposes. At most frequencies the model will have the wrong damping but the effect on the dynamic response will not be significant if the damping is light. The rate of decay of free oscillation and the frequency response curves (like those of Figure 5) for the actual damping can be estimated satisfactorily by the dashpot model if the loss factor at resonance is matched.

It is widely accepted that this procedure can be extended to model the damping in systems with many degrees of freedom. An equivalent dashpot is assigned to each natural mode in such a way that the dashpot loss factor matches the actual loss factor of the system when the system vibrates *in* that mode at the resonant frequency *of* that mode. Such a procedure neglects the possible coupling of modes due to damping. Some analytical studies of damping

coupling have been made [10, 11, 12]. Further studies may show that there are practical applications where damping coupling plays an important role in establishing a stability borderline or in influencing the partition of energy during random vibration. For the purpose of predicting stationary response levels (random or deterministic) there does not, however, seem to be any compelling practical reason within the present state-of-the art for including the additional complication of damping coupling in the mathematical model.

A more serious discrepancy between model and reality occurs when the actual damping mechanism is non-linear. Analytical treatments of non-linear damping exist [13, 14, 15], but are of quite limited scope. In practice it is common to measure or estimate the actual loss factors for amplitudes which are representative of the expected application and then to use a model with linear dashpots having these loss factors.

4. THE FREQUENCY DEPENDENT DASHPOT

When the frequency at which damping is important is known in advance, it is usually adequate to model light damping by an equivalent ideal dashpot as described in the preceding section. A more faithful model of the damping is, however, required when it is not known initially at which frequency the damping will be critical. This latter case occurs in stability analyses where the critical frequency for onset of instability is itself a sensitive function of the damping. Some examples of cases of this sort are examined in the following sections.

In order to describe a model for an actual damping mechanism like that shown in Figure 6 we use the Fourier integral to transform the time domain into a frequency domain. The Fourier transform $X(\omega)$ of a time history $x(t)$ is defined by the integral

$$X(\omega) = \int_{-\infty}^{\infty} x(t) e^{-i\omega t} \, dt \tag{9}$$

provided that $x(t)$ satisfies modest convergence and smoothness requirements [16]. The time history can be recovered from the inverse transform

$$x(t) = \frac{1}{2\pi} \int_{-\infty}^{\infty} X(\omega) e^{i\omega t} \, d\omega. \tag{10}$$

The time-domain description of the ideal-dashpot relation

$$f_d = c \frac{dx}{dt} \tag{11}$$

can be transformed into a frequency-domain relation by multiplying both sides of (11) by $e^{-i\omega t}$ and integrating to obtain

$$F_d(\omega) = i\omega c X(\omega) \tag{12}$$

where $F_d(\omega)$ is the Fourier transform of the dashpot force $f_d(t)$. Equation (12) can be interpreted as the relation between the complex amplitudes of force and displacement during cyclic oscillation at frequency ω.

For an ideal dashpot the parameter c is constant and the loss factor is given by (4). For a damping mechanism which has a different frequency dependence we can use (4) to define a frequency dependent dashpot parameter

$$c(\omega) = \frac{k\eta(\omega)}{|\omega|}. \tag{13}$$

Since the loss factors of actual damping mechanisms are almost always measured under cyclic or nearly cyclic oscillation it is appropriate to generalize (12) by inserting the frequency dependent dashpot parameter (13) to get

$$F_d(\omega) = i\omega c(\omega)\, X(\omega) = \frac{i\omega k}{|\omega|}\eta(\omega)\, X(\omega) = ik\eta(\omega)\,\mathrm{sgn}\omega\, X(\omega) \tag{14}$$

where the signum function $\mathrm{sgn}\,\omega$ takes the value $+1$ for positive ω and (-1) for negative ω (and is zero for $\omega = 0$). Equation (14) defines the behavior of a useful analytical model: a linear frequency dependent dashpot. Note that the definition is made in the frequency domain. The corresponding time-domain description is obtained by multiplying (14) by $e^{i\omega t}/2\pi$ and integrating to obtain

$$f_d(t) = \frac{1}{2\pi}\int_{-\infty}^{\infty} i\omega c(\omega)\, X e^{i\omega t}\, d\omega$$

$$= \frac{1}{2\pi}\int_{-\infty}^{\infty} i\omega c(\omega)\, e^{i\omega t}\, d\omega \int_{-\infty}^{\infty} x(\tau)^{-i\omega\tau}\, d\tau \tag{15}$$

or alternatively

$$x(t) = \frac{1}{2\pi}\int_{-\infty}^{\infty} \frac{e^{i\omega t}}{i\omega c(\omega)}\, d\omega \int_{-\infty}^{\infty} f_d(\tau)\, e^{-i\omega\tau}\, d\tau. \tag{16}$$

Unfortunately the integrals in (15) and (16) are not elementary except for rather special choices of $c(\omega)$. If $c(\omega)$ is a rational fraction of polynomials in ω^2 then the relation between $f_d(t)$ and $x(t)$ can be written as a (higher order) differential equation. This means that in place of the simple differential relation (11) for an ideal dashpot we now have a very complicated (although still linear) relationship between $f_d(t)$ and $x(t)$ for the frequency dependent dashpot.

When an ideal dashpot is placed in the oscillator in Figure 4(b) the time-domain description of the relation between the exciting force $f(t)$ and the displacement $x(t)$ is the differential equation

$$m\frac{d^2x}{dt^2} + c\frac{dx}{dt} + kx = f. \tag{17}$$

The corresponding frequency-domain description is

$$(-m\omega^2 + i\omega c + k)\, X(\omega) = F(\omega). \tag{18}$$

If now we replace the ideal dashpot (with constant c) by a frequency dependent dashpot with parameter $c(\omega)$ given by (13) the frequency-domain description becomes

$$(-m\omega^2 + i\omega c(\omega) + k)\, X(\omega) = F(\omega) \tag{19}$$

or

$$(-m\omega^2 + k[1 + i\eta(\omega)\,\mathrm{sgn}\,\omega])\, X(\omega) = F(\omega). \tag{20}$$

These frequency-domain relations are immediately useful for obtaining steady-state sinusoidal responses or stationary random response spectra. They can also be used to obtain more general response information by Fourier inversion. On occasion the following non-equations are employed to represent the inverses of (19) and (20):

$$m\frac{d^2x}{dt^2} + c(\omega)\frac{dx}{dt} + kx = f$$

$$m\frac{d^2x}{dt^2} + kx[1 + i\eta(\omega)\,\mathrm{sgn}\,\omega] = f. \tag{21}$$

These are obtained from (19) and (20) by properly inverting the inertia, stiffness and excitation terms but leaving only a mnemonic indication of the damping inverse (15) by the dubious device of mixing time-domain and frequency-domain operations. The advantage gained from the mnemonic shorthand in such non-equations is not enough to compensate for the potential confusion which they may create. The difficulty is that they *look* like equations and there is a very real danger that they *will* be interpreted literally. In the past 20 years a number [17 to 26] of ingenous, *ad hoc* rationalizations have been used to interpret non-equations of the form (21).

There are certain limitations on the frequency dependence of dashpot models if they are to represent physically realizable damping mechanisms. As we have already noted for an ideal dashpot the loss factor $\eta(\omega)$ must be a real, non-negative and even function of ω if it is to represent a loss mechanism. The frequency-dependent dashpot parameter $c(\omega)$ must likewise be real, non-negative and even. Beyond this there is the considerably more subtle causality requirement: $c(\omega)$ must be such a function of ω that the corresponding time relation represented by (16) is *causal* in the sense that the response $x(t)$ at any instant t may depend on the *previous* history of the excitation $f_d(\tau)$ for $\tau < t$ but should be independent of the *future* behavior of $f_d(\tau)$ for $\tau > t$.

Although some general theorems exist [16] it is not always easy to decide whether a given frequency function $c(\omega)$ is causal or not. In some cases it is possible to demonstrate non-causality by exhibiting a particular excitation-response pair which satisfy (16) and for which the response anticipates the excitation. This is in fact the case for the widely employed model for linear hysteretic damping in which it is assumed that the loss factor $\eta(\omega)$ is a *constant* η_0 independent of frequency. Under this hypothesis

$$c(\omega) = \frac{k\eta_0}{|\omega|} = \frac{k\eta_0}{\omega}\operatorname{sgn}\omega \tag{22}$$

and (16) reduces to

$$x(t) = \frac{1}{2\pi k\eta_0}\int_{-\infty}^{\infty}\frac{e^{i\omega t}}{i\operatorname{sgn}\omega}d\omega\int_{-\infty}^{\infty}f_d(\tau)e^{-i\omega\tau}d\tau. \tag{23}$$

If we take $f_d(t)$ to be the unit impulse $\delta(t)$ and designate the corresponding response for $x(t)$ as the impulse response function $h(t)$ it is a simple exercise in generalized limits [16, 27] to show

$$h(t) = \frac{1}{\pi k\eta_0}\frac{1}{t} \quad (-\infty < t < \infty). \tag{24}$$

This excitation-response pair, which clearly violates the causality requirement, is shown in Figure 7.

The non-causal nature of the assumption of a frequency-independent loss factor was noted independently by Fraeijs de Veubeke [28], Caughey [29] and Crandall [30]. In [30] the impulse response of a single-degree-of-freedom oscillator with small frequency-independent loss factor was calculated. The post-impulse response has the general character of a damped sinusoid but there is a small negative pre-impulse response which slowly grows from zero of $t = -\infty$ to a maximum negative value which occurs shortly after the application of the impulse (the magnitude of this maximum precursor is somewhat larger than one percent of the peak post-impulse response for the case where the loss-factor is $\eta_0 = 0{\cdot}05$).

Although there is no realizable linear damping mechanism whose loss factor is strictly independent of frequency there are many mechanisms that have loss factors which remain substantially constant within certain ranges of frequency. An example of a combined energy

storage and loss mechanism with very weak frequency dependence was given by Biot [31]. See also [29].

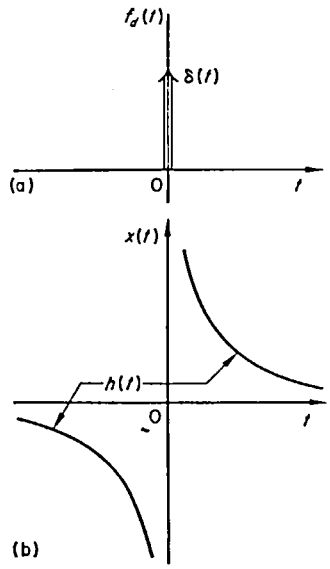

Figure 7. Example of non-causal behavior. Exciting force (a) and displacement response (b) for frequency dependent dashpot assumed to have constant loss factor at *all* frequencies.

5. DYNAMIC STABILITY OF NON-CONSERVATIVE SYSTEMS

The generally small effects of light damping become of major importance in the vicinity of resonance as we have seen. They are also of critical importance in determining stability borderlines for non-conservative systems such as flexible rotors under rotation and aero-elastic structures interacting with flowing fluid. In these systems there are generally regions (of rotational speed or fluid velocity) in which the system is stable in the sense that small disturbances decay. There may also be regions in which the system is unstable, i.e. small disturbances grow until either a non-linear limiting mechanism sets in or there is structural failure. At borderlines between stability and instability the system usually responds to a small disturbance by oscillating steadily with a small fixed amplitude. The frequency of this neutral oscillation and the location of the borderline (in terms of rotational speed or fluid velocity) can both be very sensitive to small damping in the system. In multi-moded systems the spatial distribution of damping (or equivalently the modal distribution) can have a strong influence on both of these. The frequency dependence of the damping also plays an important role in establishing the neutral stability conditions. These facts are illustrated in the examples which follow. For an extended treatment of stability of non-conservative systems see [32].

An excellent illustration is furnished by an idealized model of the classical problem of shaft whirl [33, 32]. In Figure 8 a mass point is suspended symmetrically by massless springs so that whenever the mass is displaced from the origin by a distance a there is a centrally directed restoring force of magnitude ka (independently of the rotation speed Ω of the frame). When the frame is stationary ($\Omega = 0$) the mass has two degrees of freedom in the plane of the sketch. All natural motions are linear combinations of two independent modes with the same natural frequency $\omega_n = \sqrt{k/m}$. The pair of basic modes may be taken as simple translation in the x and y directions, respectively, or (as is usually more convenient in whirling problems) as a pair of circularly polarized vibrations, one clockwise and one counterclockwise.

Furthermore, in the ideal undamped system these natural motions are completely independent of the frame rotation speed. These motions are described by the equations

$$m\begin{Bmatrix}\ddot{x}\\ \ddot{y}\end{Bmatrix}+k\begin{Bmatrix}x\\ y\end{Bmatrix}=0 \tag{25}$$

in stationary co-ordinates or by

$$m\begin{Bmatrix}\ddot{\xi}\\ \ddot{\eta}\end{Bmatrix}-m\Omega^2\begin{Bmatrix}\xi\\ \eta\end{Bmatrix}+2m\begin{bmatrix}0 & -\Omega\\ \Omega & 0\end{bmatrix}\begin{Bmatrix}\dot{\xi}\\ \dot{\eta}\end{Bmatrix}+k\begin{Bmatrix}\xi\\ \eta\end{Bmatrix}=0 \tag{26}$$

in rotating co-ordinates. Since small disturbances remain small the ideal system of Figure 8(a) is not unstable at any speed. There is, however, a latent source of instability in the centrifugal field set up by the steady rotation Ω.

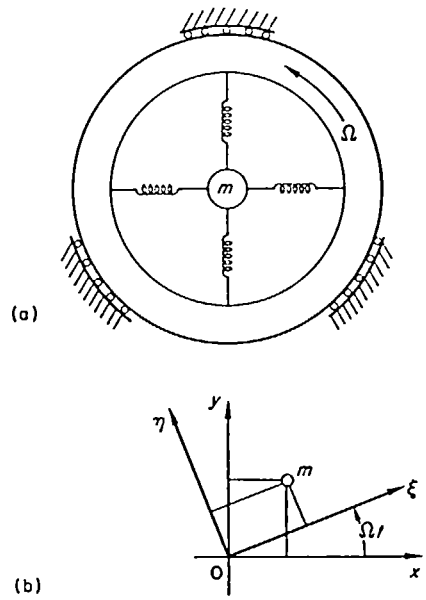

Figure 8. Model of whirling shaft. (a) Point mass m suspended by symmetrical springs from rotating frame, (b) stationary co-ordinates x, y and rotating co-ordinates ξ, η to locate mass point when displaced from origin.

Instability can be introduced by constraining the mass point to vibrate along a rotating diameter. For example, if a guide rail is installed along the ξ-axis so that η is constrained to vanish identically, equation (26) reduces to

$$m\ddot{\xi}+(k-m\Omega^2)\xi=0 \tag{27}$$

which predicts unbounded growth for ξ as soon as $\Omega^2 > k/m = \omega_n^2$, i.e. as soon as the centrifugal field overpowers the elastic field.

Now let us return to Figure 8 with two degrees of freedom and examine the effect of introducing damping. Retaining circular symmetry we still have to distinguish whether the damping of the mass is with respect to motion relative to the stationary x, y system or with respect to motion relative to the rotating ξ, η system. This can be considered as a problem of ascertaining the spatial distribution of damping. There is, however, an interaction with the frequency dependence of the damping because a whirl which appears to have the frequency ω with respect to the x, y system will appear to have the frequency $\omega - \Omega$ to an observer stationed in the rotating co-ordinate system.

A formal procedure for introducing frequency-dependent dashpots is to write time-domain differential equations for constant parameter dashpots, transform to the frequency domain and *then* replace the constant parameters by frequency dependent parameters. Thus assuming resisting forces $c_s\dot{x}$ and $c_s\dot{y}$ parallel to the *stationary* x- and y-axes and resisting forces $c_r\dot{\xi}$ and $c_r\dot{\eta}$ parallel to the *rotating* ξ- and η-axes, we can extend the undamped equations of (25) (26) to the following equations for constant-parameter dashpots. In the stationary co-ordinates we have

$$m\begin{Bmatrix}\ddot{x}\\ \ddot{y}\end{Bmatrix} + (c_s + c_r)\begin{Bmatrix}\dot{x}\\ \dot{y}\end{Bmatrix} + k\begin{Bmatrix}x\\ y\end{Bmatrix} + c_r\begin{bmatrix}0 & \Omega\\ -\Omega & 0\end{bmatrix}\begin{Bmatrix}x\\ y\end{Bmatrix} = 0, \tag{28}$$

while in the rotating co-ordinates we have

$$m\begin{Bmatrix}\ddot{\xi}\\ \ddot{\eta}\end{Bmatrix} - m\Omega^2\begin{Bmatrix}\xi\\ \eta\end{Bmatrix} + (c_s + c_r)\begin{Bmatrix}\dot{\xi}\\ \dot{\eta}\end{Bmatrix} + k\begin{Bmatrix}\xi\\ \eta\end{Bmatrix} + \begin{bmatrix}0 & -\Omega\\ \Omega & 0\end{bmatrix}\left(2m\begin{Bmatrix}\dot{\xi}\\ \dot{\eta}\end{Bmatrix} + c_s\begin{Bmatrix}\xi\\ \eta\end{Bmatrix}\right) = 0 \tag{29}$$

as equations for free damped motions with constant parameter damping (c_s with respect to the stationary axes and c_r with respect to the rotating axes).

A discussion of general solutions of these is omitted and we proceed directly to the stability borderline where a steady whirl of amplitude a is maintained. If this whirl has the (unknown) frequency ω with respect to the stationary axes then

$$x = a\cos\omega t, \tag{30}$$
$$y = a\sin\omega t,$$

and the stationary dashpot-parameter can be replaced by a frequency-dependent parameter (13) evaluated at frequency ω

$$c_s = \frac{k\eta_s(\omega)}{|\omega|}. \tag{31}$$

Viewed from the rotating axes the same whirl appears as

$$\xi = a\cos(\omega - \Omega)t, \tag{32}$$
$$\eta = a\sin(\omega - \Omega)t,$$

and the rotating dashpot parameter can be replaced by a frequency dependent parameter (13) evaluated at the frequency $\omega - \Omega$

$$c_r = \frac{k\eta_r(\omega - \Omega)}{|\omega - \Omega|}. \tag{33}$$

It is now a routine algebraic task to draw out the conditions for neutral stability from either (28) or (29). We find that neutral stability will occur if $\omega^2 = \omega_n^2$ and if the steady rotation Ω satisfies the following requirement:

$$\eta_s(\omega_n)\operatorname{sgn}\omega_n + \eta_r(\omega_n - \Omega)\operatorname{sgn}(\omega_n - \Omega) = 0. \tag{34}$$

There is no solution to (34) if $0 < \Omega < \omega_n$, but if $0 < \omega_n < \Omega$ then a solution is possible if

$$\eta_s(\omega_n) = \eta_r(\Omega - \omega_n). \tag{35}$$

The two sides of equation (35) are sketched in Figure 9. Neutral equilibrium occurs when the two curves intersect, i.e. when the stationary loss factor (at frequency ω_n) just equals the rotational loss factor (at frequency $\Omega - \omega_n$). Further study shows that the system is unstable when the rotational loss factor is greater than the stationary loss factor.

This example illustrates the remarkable fact that a stable undamped system can be made unstable by adding a damping mechanism. Actually it is only the rotational damping which

is destabilizing. Damping of motion with respect to the stationary axes always tends to stabilize the system. Damping of motion with respect to the rotating axes acts somewhat like (although not as effectively as) a diametral constraint in unleashing the centrifugal field. Viewed from the stationary axes the neutral whirl is at the natural frequency ω_n but the frequency of the whirl with respect to the rotating axes (and hence the rotation speed Ω) depends critically on the frequency dependence of the rotational damping loss factor.

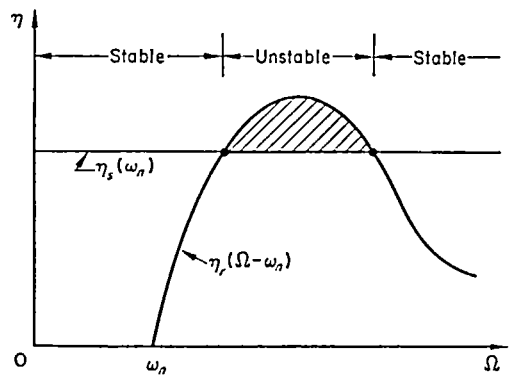

Figure 9. Location of stability borderlines according to equation (35). Neutral stability occurs at rotational speeds Ω for which rotational and stationary loss factors are equal.

The sensitivity of the location of a stability limit for small damping can be illustrated by considering what happens to Figure 9 when the damping approaches zero. A wide range of results is possible depending on the exact nature of the limiting process. For example, if η_r is allowed to vanish while η_s remains fixed, the system is *stable* for all speeds Ω and remains so when η_s is subsequently made to vanish. Alternatively if η_s is made to vanish first the system is *unstable* for all speeds Ω that are greater than ω_n. Furthermore this condition remains unchanged if subsequently the magnitude of η_r is decreased without limit. Any number of intermediate results is also possible. For example, if η_s and η_r are maintained in strict proportion as they are simultaneously brought to zero, then at any stage the unstable range will have exactly the same limits as in Figure 9.

6. FURTHER EXAMPLES

We briefly draw attention to the sensitive role of small damping in problems of internal and external flutter. Figure 10 shows an experimental set-up [34] in which a flexible cantilever tube transmits a steady flow of water. For low rates of flow the straight tube is stable with respect to small disturbances. If the flow rate is slowly increased a critical rate is reached and the pipe begins to flutter as shown in the strobe-lighted photo of Plate 2. This problem has been studied at some length [35, 36]. The sensitivity of the results to the type of damping assumed can be indicated by displaying some results from [34]. Experimental results for three different configurations are compared with analytical predictions in Figures 11 and 12. The parameter specifying the configuration of the tube-fluid system is the ratio $m_F/(m_F + m_T)$ of the fluid mass (per unit length of tube) to the total mass of fluid plus tube. At the stability borderline the important parameters are the flow velocity of the fluid V and the frequency ω of the neutral oscillation. In the experiments only the first mode loss factor was measured. The analytical results were based on a 4-mode Galerkin approximation. The first mode loss factor was put equal to the experimental value. Then two different hypotheses were made.

In the first, the loss factors of the higher modes were assumed to be *inversely* proportional to the modal natural frequencies (this would be the case if there were uniform viscous resistance to the transverse *velocity* of the tube). In the second the loss factors of the higher modes were assumed to be *directly* proportional to the modal natural frequencies (this would be the

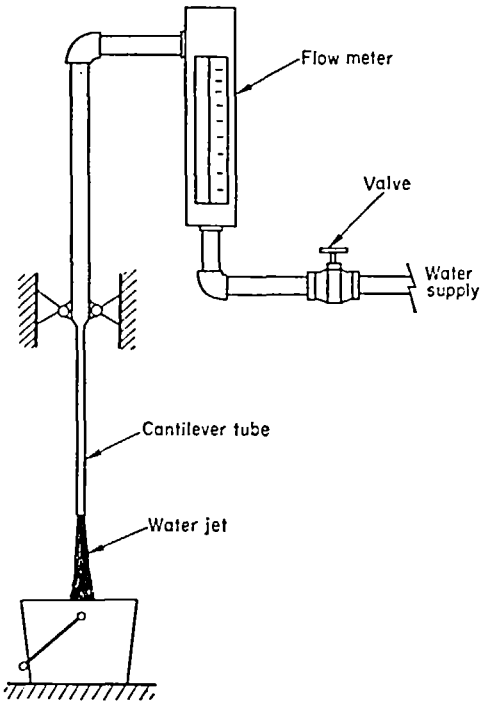

Figure 10. Flexible cantilever tube will "flutter" when flow rate surpasses critical value.

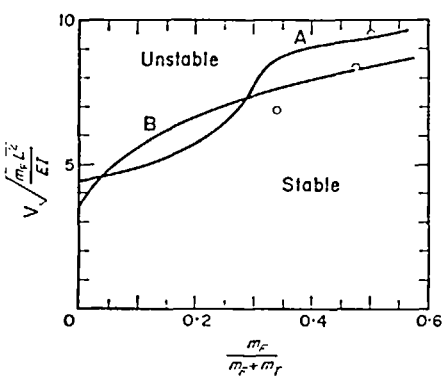

Figure 11. Stability borderlines for flow velocity. Comparison of experimental points (o) with prediction based on: A, loss factors inversely proportional to frequency; B, loss factors directly proportional to frequency. Adapted from [34].

case if resisting stresses were developed uniformly throughout the tube in proportion to the bending *strain*-rate).

In Figure 11 the predicted stability borderlines are compared with the three measured critical flow rates. In Figure 12 the measured frequencies of neutral oscillation at the stability borderline are compared with the analytical predictions. Note the wide divergence in the

two analytical models (especially for the frequency) due only to the different assumptions concerning the damping in the higher modes.

Damping also plays an important role in external flutter. For example, the problem of panel flutter due to supersonic flow over the outside face of a panel has been widely studied

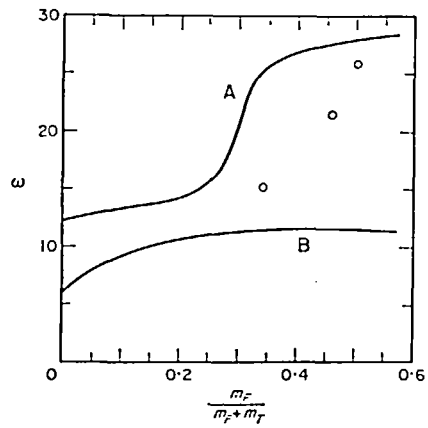

Figure 12. Frequency of neutral oscillation at stability borderline. Comparison of experimental points (o) with prediction based on: A, loss factors inversely proportional to frequency; B, loss factors directly proportional to frequency. Adapted from [34].

in recent years [37, 38]. The critical flow velocity depends on the aspect ratio of the panel, the panel boundary conditions, the magnitude of in-plane preloading and the aerodynamic damping as well as on the internal mechanical damping. The interplay between these many factors is complex. Several investigators [32, 39, 40] have noted the sensitivity of the results to the type of assumption made concerning the spatial distribution and frequency dependence of the mechanical damping.

ACKNOWLEDGMENTS

The author would like to express his thanks to L. E. Wittig for measuring the dynamic characteristics of the beam shown in Plate 1. Support for this research was provided by the National Aeronautics and Space Administration under Contract NAS 8-2504.

REFERENCES

1. C. Zener 1948 *Elasticity and Anelasticity of Metals.* Chicago: University of Chicago Press.
2. B. J. Lazan 1968 *Damping of Materials and Members in Structural Mechanics.* Oxford: Pergamon Press.
3. J. C. Heine 1966 *Thesis, Department of Mechanical Engineering, M.I.T.* The stress and frequency dependence of material damping in some engineering alloys.
4. N. Granick and J. E. Stern 1966 *Shock and Vibration Bulletin* 34, 5, 177. Material damping of aluminum by a resonant dwell technique.
5. P. M. Morse and K. U. Ingard 1968 *Theoretical Acoustics.* New York: McGraw-Hill Book Co.
6. M. Uemura and M. Takehana 1953 *Tokyo University Report, Inst. Sci., and Tech.* 7, 99. Damped vibration of thin beams (I. The effect of air resistance).
7. W. E. Baker and F. J. Allen 1957 *Aberdeen Proving Ground B.R.L. Report No.* 1033. The damping of thin beams in air.
8. W. E. Baker, W. E. Woolam and D. Young 1967 *Int. J. Mech. Sci.* 9, 743. Air and internal damping of thin cantilever beams.
9. T. K. Caughey 1963 *Random Vibration,* vol. 2, chapter 3, ed. by S. H. Crandall, Cambridge, Mass.: The M.I.T. Press. Nonstationary random inputs and responses.

10. K. A. Foss 1958 *J. appl. Mech.* **25**, 361. Coordinates which uncouple the equations of motion of damped linear dynamic systems.
11. S. H. Crandall and R. B. McCalley 1961 *Shock and Vibration Handbook*, vol. 2, chapter 28, ed. by C. M. Harris and C. E. Crede, New York: McGraw-Hill Book Co. Numerical methods of analysis.
12. T. K. Caughey and M. E. J. O'Kelly 1961 *J. acoust. Soc. Amer.* **33**, 1458. Effect of damping on the natural frequencies of linear dynamic systems.
13. T. K. Caughey 1960 *J. appl. Mech.* **27**, 649. Random excitation of a system with bilinear hysteresis.
14. S. H. Crandall, G. R. Khabbaz and J. E. Manning 1964 *J. acoust. Soc. Amer.* **36**, 1330. Random vibration of an oscillator with nonlinear damping.
15. M. R. Torres and C. D. Mote, Jr. 1969 *ASME Paper No. 69-Vibr-34*. Expected equivalent damping under random excitation.
16. A. Papoulis 1962 *The Fourier Integral and Its Applications*. New York: McGraw-Hill Book Co.
17. W. W. Soroka 1949 *J. aeronaut. Sci.* **16**, 409. Note on the relations between viscous and structural damping coefficients.
18. W. Pinsker 1949 *J. aeronaut. Sci.* **16**, 694. Structural damping.
19. R. H. Scanlan and F. W. Rosenbaum 1951 *Introduction to the Study of Aircraft Vibration and Flutter*. New York: Macmillan.
20. N. O. Myklestad 1952 *J. appl. Mech.* **19**, 284. The concept of complex damping.
21. R. E. D. Bishop 1955 *Jl R. aeronaut. Soc.* **59**, 738. The treatment of damping forces in vibration theory.
22. T. J. Ried 1956 *Jl R. aeronaut. Soc.* **60**, 283. Free vibration and hysteretic damping.
23. S. Neumark 1957 *Aero Res. Council R & M* No. 3269. Concept of complex stiffness applied to problems of oscillations with viscous and hysteretic damping.
24. P. Lancaster 1960 *Jl R. aeronaut. Soc.* **64**, 229. Free vibration and hysteretic damping.
25. R. H. Scanlan and A. Mendelson 1963 *AIAA J.* **1**, 938. Structural damping.
26. E. Skudrzyk 1968 *Simple and Complex Vibratory Systems*. Univ. Park, Pennsylvania: Pennsylvania State University Press.
27. M. J. Lighthill 1962 *Fourier Analysis and Generalized Functions*. Cambridge University Press.
28. B. M. Fraeijs de Veubeke 1960 *AGARD Manual on Elasticity*, vol. 1, chapter 3. Influence of internal damping on aircraft resonance.
29. T. K. Caughey 1962 *Proc. Fourth U.S. natn. Congr. appl. Mech.* 87, New York: ASME. Vibration of dynamic systems with linear hysteretic damping.
30. S. H. Crandall 1963 *Air, Space, and Instruments, Draper Anniversary Volume*, p. 183, ed. by S. Lees, New York: McGraw-Hill Book Co. Dynamic response of systems with structural damping.
31. M. A. Biot 1958 *Proc. Third U.S. natn. Congr. appl. Mech.* 1. New York: ASME, Linear thermodynamics and mechanics of solids.
32. V. V. Bolotin 1963 *Nonconservative Problems of the Theory of Elastic Stability*. New York: Macmillan.
33. A. L. Kimball 1924 *Gen. Elec. Rev.* **27**, 244. Internal friction theory of shaft whirling.
34. A. S. Greenwald and J. Dugundji 1967 *M.I.T. Aeroelastic and Structures Research Laboratory Report ASRL TR* 134-3. Static and dynamic instabilities of a propellant line.
35. R. W. Gregory and M. P. Paidoussis 1966 *Proc. R. Soc.* **A293**, 512. Unstable oscillation of tubular cantilevers conveying fluid, Part I—Theory, Part II—Experiments.
36. G. Herrman and S. Nemat-Nasser 1967 *Int. J. Solids and Structures* **3**, 39. Instability modes of cantilevered bars induced by fluid flow through attached pipes.
37. Y. C. Fung 1963 *AIAA J.* **1**, 898. Some recent contributions to panel flutter research.
38. J. Dugundji 1966 *AIAA J.* **4**, 1257. Theoretical considerations of panel flutter at high supersonic Mach numbers.
39. C. H. Ellen 1968 *AIAA J.* **6**, 2169. Influence of structural damping on panel flutter.
40. C. P. Shore 1969 *NASA TN D-4990*. Effects of structural damping on flutter of stressed panels.